Hydrogen-Rich and Clean Fuel Gas Production from Co-pyrolysis of Biomass and Plastic Blends with CaO Additive

Yuanjun Tang, Jun Dong, Yuan Zhao, Guoneng Li, Yong Chi, Elsa Weiss-Hortala, Ange Nzihou, Guanqun Luo, Chao Ye

Hydrogen-Rich and Clean Fuel Gas Production from Co-pyrolysis of Biomass and Plastic Blends with CaO Additive

Yuanjun Tang,* Jun Dong, Yuan Zhao, Guoneng Li, Yong Chi, Elsa Weiss-Hortala, Ange Nzihou, Guanqun Luo, and Chao Ye

Cite This: https://doi.org/10.1021/acsomega.2c04279

Read Online

ACCESS | Metrics & More | Article Recommendations

ABSTRACT: The treatment and disposal of waste biomass and plastics are of great importance to achieve both waste management and resource recycling. In this work, pyrolysis of biomass and plastic blends were investigated to identify the influence of temperature and in situ CaO addition on the production of hydrogen-rich, HCl-free, and low tar content fuel gases. The results show that the increase in temperature and the use of CaO significantly improved both the quantity and quality of the fuel gas and mitigated the formation of tar compounds and HCl. Moreover, H_2 yield was significantly improved from 0.30 to 3.68 mmol/g with the increase in temperature from 550 to 850 °C. Also, the use of in situ CaO significantly increased the H_2 yield by 28−88%. The H_2/CO ratio was also enhanced from 0.35 to 1.50 with the temperature increase and CaO addition. Tar removal efficiency reached approximately 70.09% with the use of CaO at 850 °C. The produced HCl gas could be effectively absorbed by CaO through dechlorination reactions to form CaClOH at a highest mitigation efficiency of 92.37%. The results could be used to develop clean and efficient treatment technologies of waste biomass and plastics.
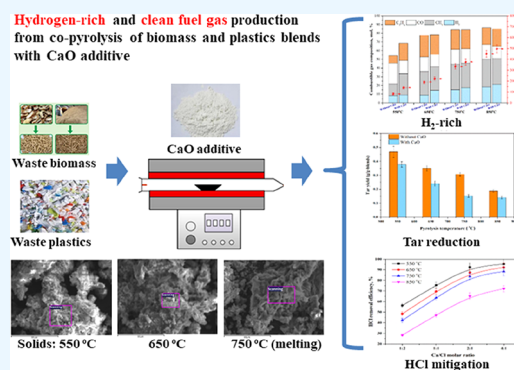
1. INTRODUCTION

The continuous increase in energy demand and the growing awareness about the environment have accelerated the growth of waste biomass and plastics management in China. Besides being treated as an environmental burden, waste biomass and plastics are also considered useful resources, supplying energy or serving as raw materials.[1] Direct combustion of waste biomass and plastics is an effective method to realize waste disposal and energy recovery. Nevertheless, incineration of waste biomass or plastics has inevitable drawbacks of corrosion issues and toxic emissions, particularly acidic gases, dioxins, or heavy metals.[2,3]

Co-pyrolysis of waste biomass and plastics is among the potential alternatives to achieve both clean and efficient treatment and energy recovery.[4−8] Instead of being all converted into thermal energy of flue gas, waste biomass and plastic blends are converted to value-added intermediates (such as fuel gas, solids, or oil) during pyrolysis.[9−11] The intermediates can subsequently be stored, transported, or utilized in more environment-friendly and energy-efficient downstream pathways. Therefore, more research attention has been paid to pyrolysis-based technologies in recent years.[4,12,13]

Pyrolysis is widely recognized as the most primary step of waste thermal conversion and affects the yields and properties of the products in the initial stage. Therefore, the investigation of waste biomass and plastic blends pyrolysis is of great importance and meaningful to understanding the thermochemical conversion of combustible solid wastes. Co-pyrolysis of waste biomass and plastic blends has become a more and more popular research topic in the field of waste management. Publications focused on the pyrolytic performances that are affected by reactor types,[14,15] reaction temperature,[16,17] reaction pressure,[18] residence time,[19,20] and heating methods.[21,22] Besides, co-pyrolysis of the blends offers a green and sustainable route for the generation of H_2, which is considered the most important energy carrier for future societies.[23,24] However, the formation of tar compounds and high CO_2 content in the produced pyrolytic gases significantly limit the commercial applications of waste pyrolysis technologies.[25] Moreover, the presence of chlorine in waste plastics (e.g., in PVC and rubber) would generate HCl in gaseous products, causing severe corrosion issues and accelerating the formation of toxic organic compounds. Therefore, the quality of produced fuel gas needs to be enhanced.

Table 1. Composition and the Ultimate and Proximate Analyses Results for the Waste Biomass and Plastic Blends

mass percentage of waste biomass and plastic blends				
biomass (ar[a], wt %)			plastics (ar[a], wt %)	
flour	paper	wood	polyethene (PE)	polyvinylchloride (PVC)
55.0	15.0	5.0	15.0	10.0

mass percentage of waste biomass and plastic blends									
proximate analysis (ad[a], wt %)				ultimate analysis (ad[a], wt %)					
moisture	ash	volatile	fixed carbon	C	H	O[b]	N	S	Cl
5.2	3.0	77.1	14.7	47.5	6.0	30.3	1.1	0.3	6.6

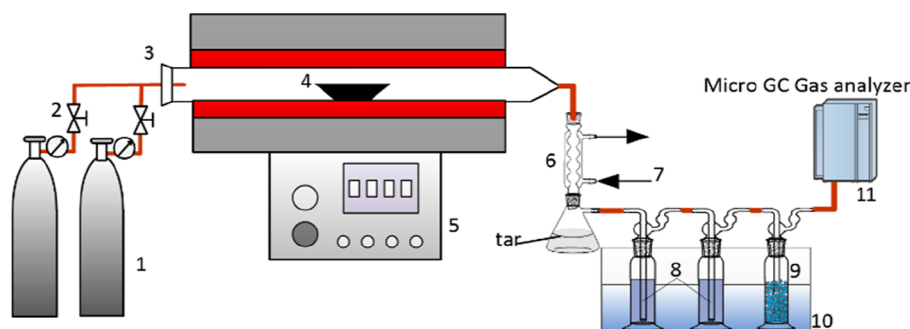[a]ar means as received basis, and ad refers to air-dried basis. [b]By difference.

Figure 1. Schematic diagram of the experimental facility: 1, high-pressure gas cylinder; 2, flow meter; 3, reactor; 4, quartz boat; 5, controller; 6, condenser; 7, cooling water; 8, impingers with 0.1 mol dm^{-3} NaOH solution; 9, impinger with silica gel; 10, ice-bath cooler; and 11, micro-GC gas analyzer.

Catalysts or additives are commonly used to enhance the quality of pyrolytic gas by cracking tar compounds, absorbing CO_2, and mitigating HCl contained in the produced fuel gases.[26−30] Among the auxiliaries, calcium-based additives (e.g., calcium oxide, calcium hydroxide, and calcium carbonate) are the most preferable substances used to achieve the abovementioned aims. This is mainly due to the properties of low price and vast abundance on the earth of calcium-based additives. Among which, calcium oxide (CaO) is the most commonly used additives in many scenarios, and it plays important roles during waste biomass and plastic co-pyrolysis.[31] On the one hand, CaO can be regarded as efficient CO_2 absorbents and H_2 production adjusters to enhance the quality of produced fuel gas by accelerating water−gas shift reactions.[32] On the other, it can inhibit the formation of tar compounds in the produced fuel gas through tar catalytic thermal cracking.[28,33,34] Furthermore, Ca-based additives are also used either directly in the furnace or in air pollution control systems for acid gas removal, such as the desulfurization process, which is employed in most of the coal-fired power plants. For the same reason, CaO can also serve as potential in situ reactants to mitigate HCl. The reason is because Ca-based additives can immobilize chlorine through heterogeneous gas−solid reactions to form solid-phase products, such as $CaCl_2$ or CaClOH.

Accordingly, this study aimed to investigate the triple effects of reaction temperature and in situ CaO additive on: (1) the formation of H_2-rich and low CO_2 content fuel gas; (2) the reduction of tar compounds; and (3) the mitigation of HCl in the produced fuel gas during co-pyrolysis of waste biomass and plastic blends. It is expected that the knowledge obtained in this work can serve as a piece of fundamental understanding for the identification of more energy-efficient and environ-ment-friendly thermal conversion techniques of waste biomass and plastics in China.

2. MATERIALS AND METHODS

2.1. Waste Biomass and Plastic Blends and CaO Characteristics. To maintain the consistency of feedstock in the experiments, artificial waste biomass and plastic blends were used in all the experiments. It was prepared to match the typical waste biomass and plastic proportions in municipal solid waste in Hangzhou, China. The physical composition and the ultimate and proximate analyses results are presented in Table 1. Before the experiments, the blends were ground and sieved to particle sizes of below 1.00 mm. The CaO additive was prepared to size in the range of 0.25−0.43 mm and calcined at 850 °C for 2 h. The prepared CaO additive had the specific surface area, total pore volume, and average pore diameter of 2.37 m^2/g, 0.039 cm^3/g, and 25.0 nm, respectively.

2.2. Test Facilities and Procedures. An experimental laboratory setup, mainly consisting of a tubular furnace unit, a gas source unit, and a sampling unit, was employed to study the influence of temperature and the addition of CaO on the thermal conversion behavior and HCl mitigation during the co-pyrolysis of waste biomass and plastic blends. The system is shown in Figure 1. High purity nitrogen gas with a flow rate of 120 mL/min was supplied as the carrier gas using a high-pressure gas cylinder. The tubular furnace reactor was electrically heated with an electrical power of 5.0 kW. A K-type thermocouple was inserted in the middle of the heating area to control and record the temperature profile. The reaction zoom was made of a quartz tube with a length of 700.0 mm and a diameter of 40.0 mm. A water-cooled condenser was used after the reactor to collect the liquid condensates. Three ice-bath-cooled impingers were used to collect HCl gas and to remove moisture (water). The first two

impingers contained 0.1 mol dm^{-3} sodium hydroxide solution, whereas the third one contained silica gel for moisture removal.

Before the experiments, the quartz tubular furnace was preheated to the desired temperature via electrical heating. Once the temperature stabilized, the quartz boat, with 5.0 g of biomass and plastic blends and CaO additive (0.26 g for Ca/Cl molar ratio of 1:2; 0.52 g for 1:1; 1.04 g for 2:1; and 2.08 g for 4:1) was uniformly mixed together and then pushed into the center of the reactor quickly to avoid air leakage. The reaction time (30 min) was the same for all the experiments. Solid residues and liquid products were accurately measured by weighing the quartz boat and the condenser, respectively. HCl gas was absorbed by the solutions through the gas trapping route.

2.3. Analysis Method. The composition of the produced gas was analyzed using a micro gas chromatograph analyzer (micro gas chromatograph 490 analyzer, Agilent). The produced fuel gas contained H_2, CO, CH_4, C_2H_m (the sum of C_2H_2, C_2H_4, and C_2H_6), CO_2, and N_2. The analyzer was equipped with 10 m MS5A, 10 m PPU, and 8 m 5CB (columns) with helium as the carrier gas. The total gas yield was quantified based on a N_2 balance by comparing the N_2 concentration in inlet and production gases. The concentration of HCl gas was detected using an ion chromatograph (Thermo Fisher Scientific, Integration). Liquid products were collected from the condenser and by washing the reactor walls and connecting pipes. Tar composition was identified using gas chromatography–mass spectrometry (Agilent 8860-5977B). Solid products were collected from the quartz boat after each experiment. Also, they were detected using X-ray diffraction (XRD, D8 Advance Bruker) and SEM (Carl Zeiss, Ultra 55). For experiments with CaO addition, the mass of additionally added CaO was subtracted from the solid products.

To evaluate the quality of the produced fuel gas, the carbon conversion efficiency (η_C) is determined using eq 1 as

$$\eta_C = \frac{\text{total gas yield} \times (yCO + yCO_2 + yCH_4 + 2 \times yC_2H_m) \times 12}{22.414 \times \text{mass of carbon in the blends}}$$
$$\times 100\% \tag{1}$$

where yCO, yCO_2, yCH_4, and yC_2H_m are the molecular fractions of CO, CO_2, CH_4, and C_2H_m in the produced fuel gas.

The effect of the increase in temperature and the use of in situ CaO additive on the removal efficiency of condensate compounds were measured by thermal removal efficiency of tar (T_tRE) and catalytic removal efficiency of tar (T_cRE), which are given by eqs 2 and 3, respectively.

$$T_tRE = \left(1 - \frac{\text{tar yields without CaO}}{\text{tar yield without CaO at 550 °C}}\right) \times 100\% \tag{2}$$

$$T_cRE = \left(1 - \frac{\text{tar yields with CaO}}{\text{tar yield without CaO at 550 °C}}\right) \times 100\% \tag{3}$$

The effect of CaO on the mitigation of HCl was determined using the mitigation efficiency of HCl (HME) by eq 4

HCl mitigation efficiency

$$= \left(1 - \frac{\text{HCl generation with CaO}}{\text{HCl generation without CaO}}\right) \times 100\% \tag{4}$$

To make sure of the reliability and reproducibility of the experimental results, all the experiments were repeated thrice, and the results reported in the present work are the average values. The mass balance of the solids, liquids, and gases reached 85−96% for all the experimental runs.

3. RESULTS AND DISCUSSION

3.1. Mass Distribution of Pyrolytic Products. Figure 2 shows the increase in temperature and the use of in situ CaO
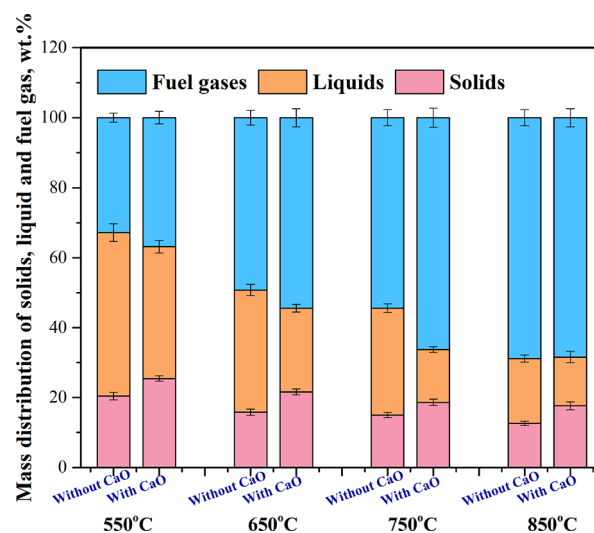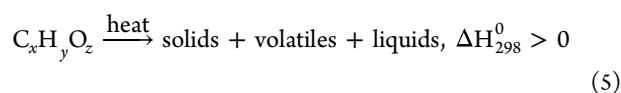

Figure 2. Effect of the increase in temperature and the presence of in situ CaO additive on mass distribution of pyrolysis products (Ca/Cl molar ratio = 1:1).

additive on the mass distribution of pyrolysis products. Temperature is one of the determinant factors affecting the pyrolytic reactions. It significantly influences the yields of the produced gas, solid residues, and liquid products from the co-pyrolysis of waste biomass and plastic blends. The results showed that higher temperatures improved the generation of produced gas (continuously increased from 32.8 to 68.6% within the experimental temperature range of 550−850 °C) and simultaneously decreased the yield of solid residues and liquid products. The mass percentage of solids declined slightly from 20.4 to 12.6%, whereas the liquid yields sequentially reduced from 46.8 to 18.6% with increased temperature. The results were in good agreement with previous findings.[35−37] It is well recognized that changing the temperature will significantly affect the chemical reaction results due to the shift of the thermodynamic equilibria. For the co-pyrolysis of the blends, higher temperatures favor the devolatilization at the initial stage of the reactions, as shown by eq 5. Meanwhile, higher temperatures also significantly accelerated the thermal cracking reactions of condensate liquids to form incondensable light hydrocarbons or gases (as given by eq 6).
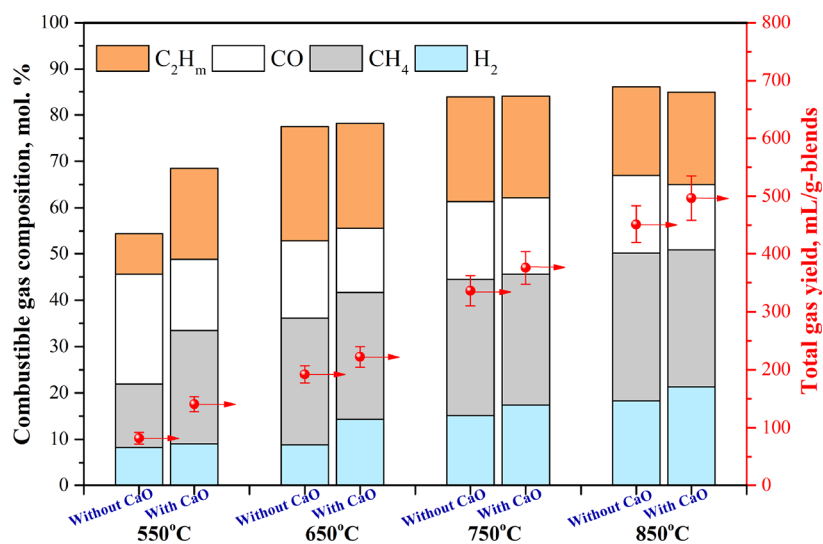
$$C_xH_yO_z \xrightarrow{\text{heat}} \text{solids + volatiles + liquids}, \Delta H^0_{298} > 0 \tag{5}$$

Figure 3. Effect of the increase in temperature and the use of in situ CaO on the composition of produced combustible gases and the yield of total fuel gas (Ca/Cl molar ratio = 1:1).
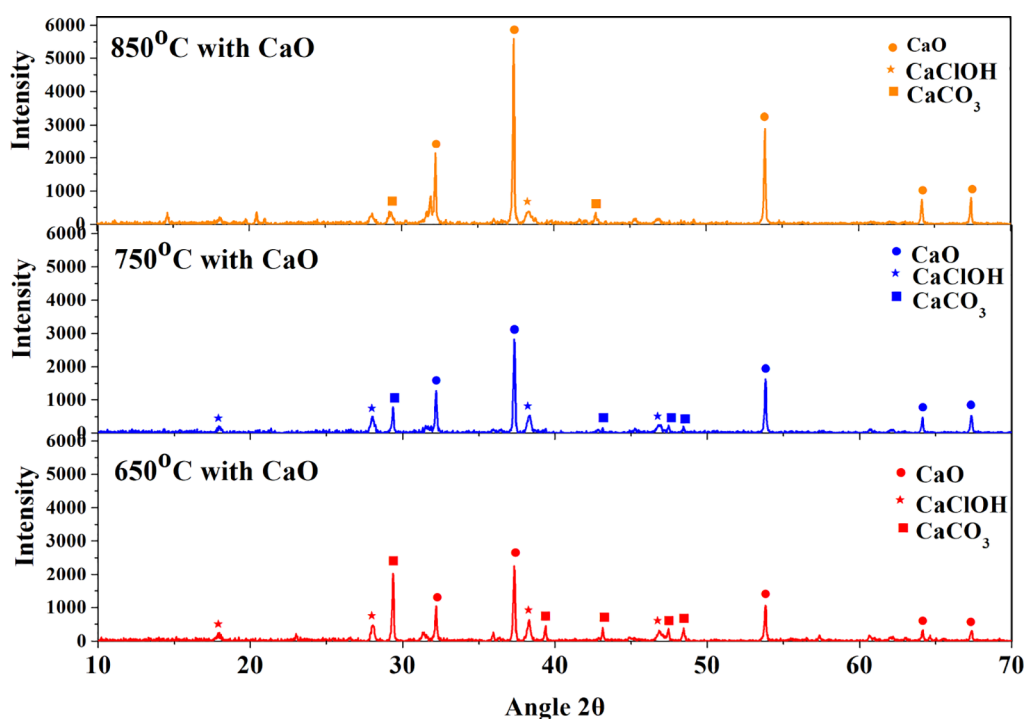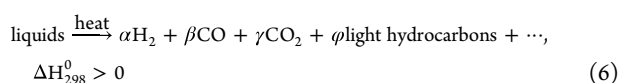

Figure 4. Effect of the increase in temperature and the use of in situ CaO on solid products.

$$\text{liquids} \xrightarrow{\text{heat}} \alpha H_2 + \beta CO + \gamma CO_2 + \varphi \text{light hydrocarbons} + \cdots,$$
$$\Delta H^0_{298} > 0 \tag{6}$$

Concerning the influence of CaO additive, the use of CaO decreased the yields of liquid product by around 4.6−15.4% within the studied experimental temperature, but increased the generation of both the solid residues (by 3.6−5.8%) and produced fuel gas (by −0.4 to 11.8%). Similar results were reported in the literature, indicating that the addition of in situ CaO during the pyrolysis of waste biomass and plastics significantly enhances the catalytic thermal cracking reactions of tar compounds, leading to the conversion of liquid condensates to incondensable gases and light hydrocarbons, as shown by eq 7.[26,28,31,38] Regarding the solid products, due to

the presence of CaO additive, some acidic gases, especially CO_2 and HCl were immobilized in the solid residues and thus the yield increased by a slight bit.

$$\text{liquids} \xrightarrow{\text{CaO additive}}$$
$$\alpha H_2 + \beta CO + \gamma CO_2 + \varphi \text{light hydrocarbons} + \cdots \tag{7}$$
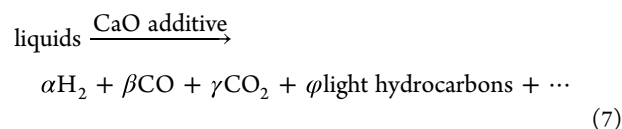
3.2. Generation of Hydrogen-Rich Fuel Gas.
3.2.1. Combustible Fuel Gas Properties. Figure 3 shows the effect of temperature and CaO additive on the yield of total fuel gas and the combustible gas composition (i.e., H_2, CH_4, CO, and C_2H_x). The results show that, with the increase in temperature from 550 to 850 °C, the yield of total fuel gas

improved significantly from 81.9 mL/g-blends to 451.4 mL/g-blends. Meanwhile, the molecular fraction of H_2 and CH_4 continuously increased from 8.3 to 18.3% and from 13.7 to 31.8%, respectively. It is mainly due to the enhancement of endothermic devolatilization and the degradation of condensates (as presented in eqs 5 and 6) at higher temperatures to generate more combustible gases. The content of carbon monoxide (CO) in the fuel gas fluctuated within the range of 16.7−23.6% under the experimental temperatures. The reason is mainly attributed to the competing reactions among the degradation of condensates (eq 6), the water−gas reaction (eq 8), and the water−gas shift reaction (eq 9) to either generate CO or consume CO.[39] Similar findings were reported in the literature.[40] Regarding C_2H_m (the sum of C_2H_2, C_2H_4, and C_2H_6), the fraction of C_2H_m increased rapidly from 8.8 to 24.7% when the experimental temperature increased from 550 to 650 °C. However, when the temperature is further increased, the content of C_2H_m reduced to 19.1% at 850 °C. The increase of C_2H_m fraction at the initial stage was mainly due to the acceleration of condensates' thermal cracking to generate more light hydrocarbons with the increase in temperature (eq 6). However, a further increase in the temperature favored the reforming reactions of hydrocarbons (as shown by eq 10), which resulted in the consumption of C_2H_m at higher temperatures.

$$C + H_2O \rightarrow CO + H_2, \quad \Delta H_{298}^0 = 131.3 \text{ kJ/mol} \tag{8}$$

$$CO + H_2O \rightarrow CO_2 + H_2, \quad \Delta H_{298}^0 = -41 \text{ kJ/mol} \tag{9}$$

$$C_nH_m + 2nH_2O \rightarrow nCO_2 + \left(2n + \frac{m}{2}\right)H_2, \; \Delta H_{298}^0 > 0 \tag{10}$$
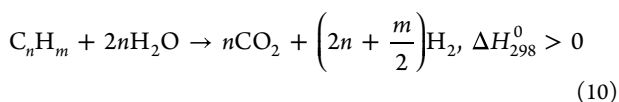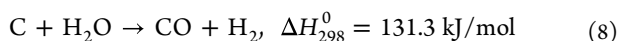
The influence of in situ CaO additive on the production of fuel gas and the composition of combustible gases were also investigated, and the corresponding results are shown in Figure 3. The yield of the total fuel gas ranged from 140.7 to 496.74 mL/g-blends with the presence of in situ CaO at the studied temperature range and increased by 10.1−71.9% as compared to the conditions without CaO. Furthermore, the content of H_2 gas was promoted by adding CaO, though the generation of CO was inhibited. This can be attributed to the acceleration of the water−gas shift reaction (as shown by eq 9). With the addition of CaO, the produced CO_2 was absorbed through the carbonation reaction to form $CaCO_3$. The consumption of CO_2 would thus lead to the acceleration of eq 9 to produce more H_2 and consume more CO. This fact was confirmed by the XRD results as presented in Figure 4, which revealed the formation of $CaCO_3$ from CaO with the produced CO_2 gas. The results show that more $CaCO_3$ was formed at lower experimental temperatures. When the temperature was increased, the intensity of XRD results declined sharply. This is connected with the thermal decomposition of the produced $CaCO_3$ at higher temperatures, which will result in the decomposition of the produced $CaCO_3$.

Regarding light hydrocarbons (CH_4 and C_2H_m), the content increased dramatically by approximately 21.7% with CaO addition at a low temperature of 550 °C. This reason is mainly attributed to the enhancement of catalytic cracking of the liquid condensates (eq 6). However, at higher temperatures of 650−850 °C, the molar fraction of light hydrocarbons reduced by around 1.6−2.1% with the addition of CaO, the reason is

due to the strength of the reforming reactions of hydrocarbons by CaO (eq 10).

3.2.2. Carbon Conversion Efficiencies. Carbon conversion efficiency reflects the molecular fraction of carbon originating from the feed and getting converted into the fuel gas as expressed in eq 1. As demonstrated in Figure 5, the increase in
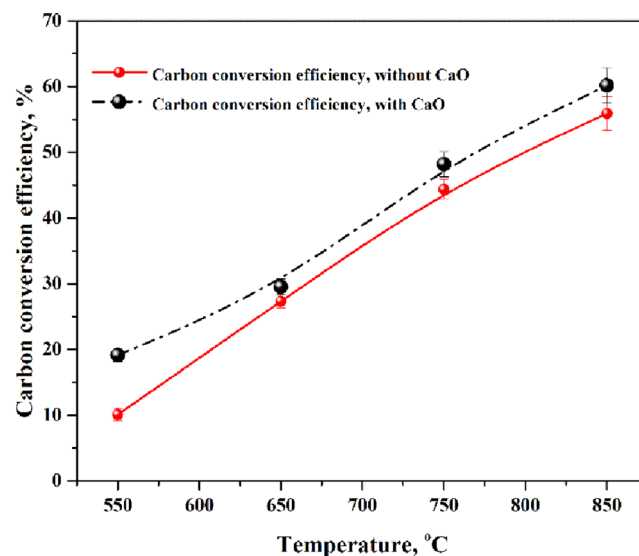

Figure 5. Carbon conversion efficiency from the feedstock to the produced fuel gas.

reaction temperature and CaO favored the transfer of carbon from the waste biomass and plastic blends to the produced gas. Carbon conversion efficiency was increased from 10.11% under the condition of 550 °C without CaO to 60.13% under the condition of 850 °C with CaO additive.

3.2.3. Hydrogen Yield and H_2/CO Ratio. The production of H_2 gas and the molecular ratio of H_2/CO are vital indicators to demonstrate the quality of fuel gas and determine directly its further applications. The more the H_2 was obtained, the higher the fuel gas quality could be expected. It is reported that, with the increase in the H_2/CO ratio, the produced fuel gas could be utilized in Fischer−Tropsch process (with Fe- and Co-based catalyst) (H_2/CO within the range of 0.5−1.5), Fischer−Tropsch synthesis (H_2/CO within the range of 1.5−3.0), gas turbine combustion (H_2/CO within the range of 2.5−4.0), or solid oxide fuel cells (H_2/CO within the range of 4.0−6.0).[41,42] Therefore, the variations in the yield of H_2 and the ratio of H_2/CO as functions of temperature and CaO additive are presented in Table 2. When the pyrolysis temperature varied from 550 to 850 °C, the production of H_2 improved dramatically from 0.30 to 3.68 mmol/g-blends.

Table 2. Effect of the Increase in Temperature and the Use of In situ CaO on the Yield of H_2 Gas and the Molecular Ratio of H_2/CO

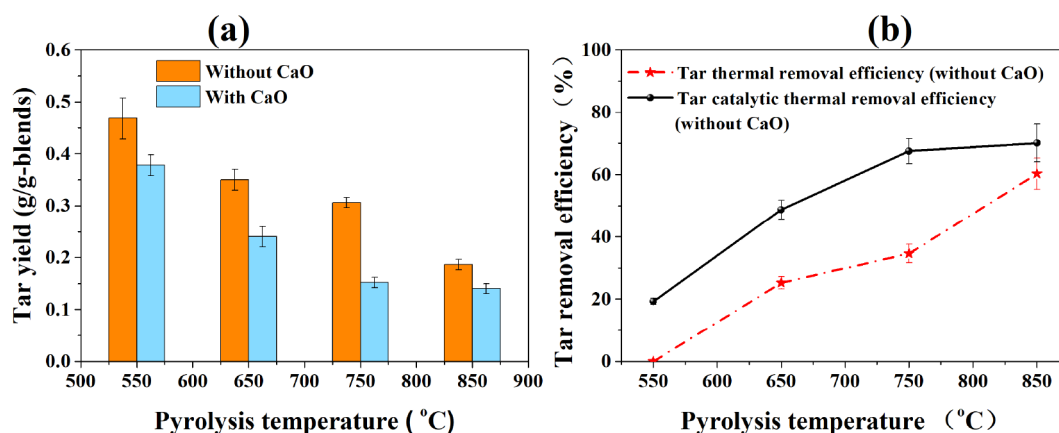|	without CaO		with CaO (Ca/Cl = 1:1)	
	H_2 yield (mmol/g-blends)	H_2/CO ratio	H_2 yield (mmol/g-blends)	H_2/CO ratio
550 °C	0.30	0.35	0.57	0.59
650 °C	0.76	0.53	1.42	1.03
750 °C	2.27	0.90	2.92	1.05
850 °C	3.68	1.09	4.72	1.50

Figure 6. Tar yields and tar removal efficiencies under the experimental conditions (Ca/Cl molar ratio = 1:1): (a) tar yield and (b) tar removal efficiency.
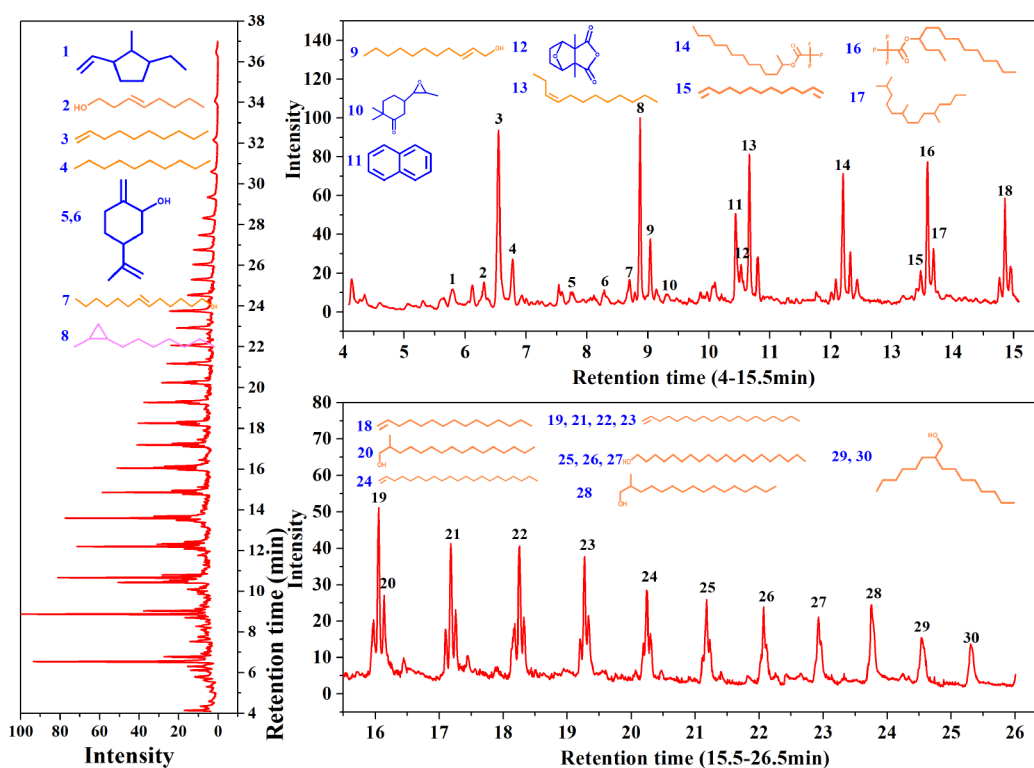

Figure 7. Characterization of tar compounds at 550 °C.

Meanwhile, the molecular ratio of H_2/CO increased from 0.35 to 1.09. The reason is mainly attributed to the enhancement of the devolatilization of waste biomass and plastics and also the degradation of condensates to generate more H_2 under higher temperatures.

With regards to CaO additive, the use of in situ CaO significantly enhanced the yield of H_2 (from 0.57 to 4.72 mmol/g-blends) as well as the H_2/CO ratio (from 0.59 to 1.50), revealing a significant enhancement in the produced fuel gas quality through the addition of in situ CaO. The acceleration of the water–gas shift reaction is responsible for this phenomenon. Furthermore, it is also worth mentioning that, under 850 °C and with CaO addition, the generated syngas could directly be used in Fischer–Tropsch synthesis because a remarkable higher H_2/CO ratio of 1.5 was obtained under such circumstances.

3.3. Generation of Clean Fuel Gas. *3.3.1. Tar Compound Mitigation.* One of the most serious bottlenecks in the utilization of pyrolytic fuel gas is the formation of tar compounds (i.e., the liquid condensates). Tar compounds may not only block or damage the devices but also limit further utilization of the products. Therefore, the yield and thermal/catalytic thermal removal efficiency of tar were determined and the corresponding results are presented in Figure 6. The results show that the increase in temperature and the use of in situ CaO additive sharply reduced the formation of condensates in the products during the pyrolysis of waste biomass and plastic blends. It is well known that the decomposition of tar occurs through two pathways: one is thermal cracking (eq 6), and the other is catalytic cracking (eq 7). As shown in Figure 6a, the content of tar declined dramatically from 0.47 g/g-blends at 550 °C to 0.19 g/g-blends at 850 °C without CaO additive.
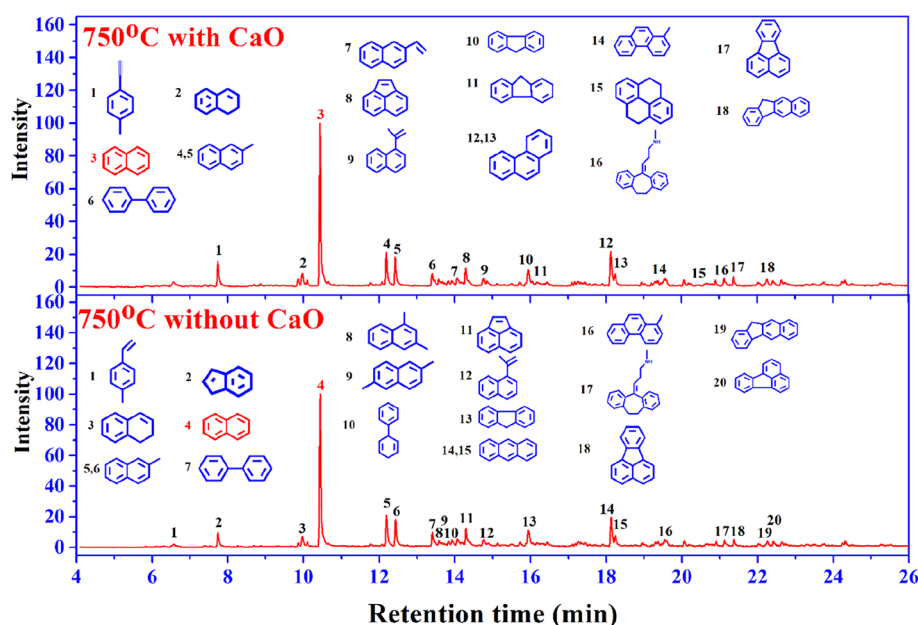
Figure 8. Characterization of tar compounds at 750 °C with CaO (Ca/Cl molar ratio = 1:1) and without CaO.

This is mainly attributed to the increase in temperature, which accelerated the degradation of condensates to light hydrocarbons. With the presence of CaO, the content of tar further decreased from 0.38 to 0.14 g/g-blends when the temperature was varied in the range of 550−850 °C. This is mainly due to the presence of O^{2-} ions on the active sites of CaO's surface, which destabilized the spatial stability of π-electron clouds of the aromatic ring structures and promoted the ring-opening reactions of aromatic compounds, thus achieving the catalytic degradation of tar.[38,43,44]

Figure 6b reports the thermal and catalytic removal efficiencies of tar compounds during the pyrolysis of the blends. According to eqs 2 and 3, tar yield at 550 °C without CaO addition was set as the baseline. The results show that tar thermal removal efficiency (T_tRE) continuously increased from 25.2 to 60.3% with the increase in pyrolysis temperature from 650 to 850 °C, which means more than half of the generated tar under low experimental temperature (baseline) would be decomposed at a higher temperature of 850 °C. The in situ CaO addition enhanced tar removal efficiency by promoting catalytic cracking (eq 7). Compared to the thermal removal efficiency of tar, a 9.8−32.9% increment in tar catalytic thermal removal efficiency (T_cRE) was obtained. It is worth mentioning that the effect of CaO on the catalytic thermal cracking of tar decreased gradually with the increase in temperature. Within the temperature range of 550−750 °C, the catalytic removal efficiency of tar increased significantly from 19.2 to 67.5%. However, when the temperature was further increased to 850 °C, the increase in T_cRE was limited only at around 2.5%. This was because under higher experimental temperature, a large portion of tar compounds had already decomposed due to thermal cracking, so the effect of CaO as a catalyst for catalytic cracking was not apparent. Meanwhile, CaO properties (pore structure and specific surface area) at higher temperatures might have degraded due to sintering and carbon deposition at higher temperatures.

Figures 7 and 8 show the characterization results of the tar compounds at temperature of 550 and 750 °C with/without CaO addition. Results reveal that at lower pyrolysis temper-

ature of 550 °C, the main pyrolytic tar compounds were chain hydrocarbons. The reason is mainly due to the content of plastics in the blends (15% PE and 10% PVC). Plastics are easily decomposed at low temperatures and generate a large number of chain hydrocarbons, especially olefins, due to the fracture of polymer carbon chains. However, at a higher pyrolysis temperature of 750 °C, the main compounds changed to aromatic hydrocarbons, and no chain hydrocarbons were detected. The reasons are mainly composed of two aspects: on the one hand, higher temperature promotes the decomposition and reforming of aliphatic chain hydrocarbons to form light gases, such as CH_4, H_2, CO, and CO_2 and on the other hand, at higher temperatures, chain hydrocarbons undergo dehydrogenation and cyclization to form aromatic compounds.

3.3.2. HCl-Free Gas Production. Beside tar compounds, Cl-containing contaminants are also key obstacles for the clean and efficient utilization of pyrolytic fuel gases, especially for waste plastics with high chlorine content (e.g., PVC). The use of in situ CaO could react with HCl gas to generate CaClOH (see XRD spectra shown in Figure 4), thus preventing the release of chlorine into the produced fuel gas. Therefore, the effect of temperature and the use of in situ CaO on the mitigation of HCl gas were also considered in the present work.

The HCl mitigation efficiency as a function of temperature and Ca/Cl molecular ratio was investigated and the corresponding results are illustrated in Figure 9. The results show that the variation of temperature from 550 to 850 °C had an adverse impact on the mitigation of HCl gas by CaO addition. For the molecular ratio of Ca/Cl at 2/1, the value of the mitigation efficiency of HCl (HME) decreased continuously from 92.4 to 65.2%. It is worth mentioning that the decrease of HME value was accelerated at higher temperatures. HME value decreased by 8.8% in the temperature range of 550−750 °C; whereas, it reduced sharply by 18.3% when the temperature was further increased to 850 °C. This can be explained from two aspects. On the one hand, according to Shemwell et al.,[45] the binding energy of the in situ CaO
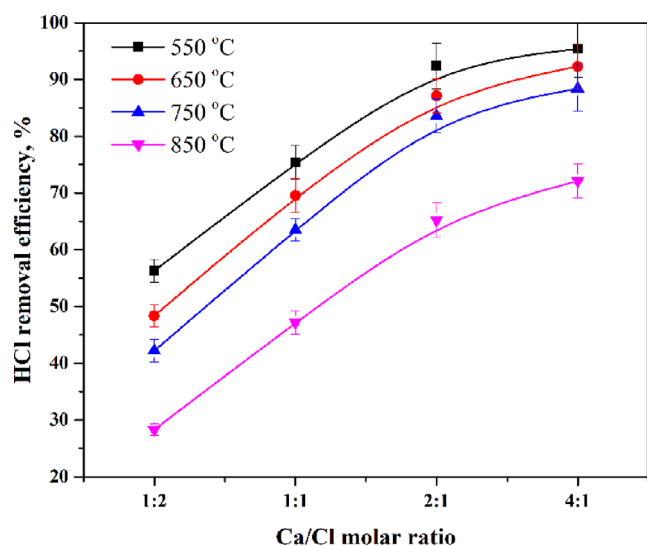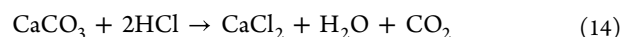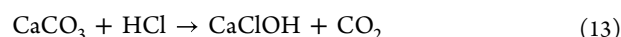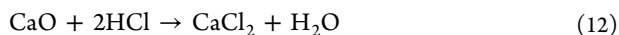
Figure 9. Effect of the increase in temperature and the molecular ratio of Ca/Cl on the mitigation efficiency of HCl gas.

additive and the produced HCl gas was decreased at higher temperatures because of the variation of the chemical equilibrium constant of dechlorination reactions (eqs 11−14),[46] therefore the dechlorination reactions were limited at higher temperatures. On the other hand, at a temperature higher than 750 °C, surface melting of dechlorination products occurred (i.e., the melting temperature of $CaCl_2$ was 772 °C[47]).

$$CaO + HCl \rightarrow CaClOH \quad (11)$$

$$CaO + 2HCl \rightarrow CaCl_2 + H_2O \quad (12)$$

$$CaCO_3 + HCl \rightarrow CaClOH + CO_2 \quad (13)$$

$$CaCO_3 + 2HCl \rightarrow CaCl_2 + H_2O + CO_2 \quad (14)$$

Regarding the influence of the molecular ratio of Ca/Cl, the stoichiometric molecular ratio of Ca/Cl should be 1/2 or 1/1, depending on the final products $CaCl_2$ or CaClOH, respectively. However, the HME value under such conditions was relatively low and ranged only from 42.2 to 69.6%. This means that the overuse of CaO additive was essential to achieve acceptable HME levels. Meanwhile, at 750 °C, the HME value increased dramatically by around 41.2% when the molecular ratio of Ca/Cl was increased from 1/2 to 2/1. However, further increase in the molecular ratio to 4/1 resulted in a limited increment of HME by approximately 4.8%. Therefore, in this work, the molecular ratio of Ca/Cl at 2/1 was considered the most appropriate proportion of in situ CaO to mitigate HCl. The optimal working condition was obtained at 750 °C (from the gas quality perspective) and the molecular ratio of Ca/Cl at 2/1 (from the HME perspective). In this case, the HCl gas mitigation efficiency reached 83.6%. It also has to be clarified that the amount of CaO added into the tubular furnace did not utterly equal the amount of the CaO reacted. Therefore, in this work, the molar ratio, as well as the stoichiometric amount of CaO indicates only the amount of CaO added to the system.

The results from XRD spectra further confirmed the dechlorination results. As shown in Figure 4, the obtained minerals mainly included $CaCO_3$, CaO, and CaClOH. The only Cl-containing solid product detected was CaClOH, which means eqs 11 and 13 were the main dechlorination reactions in the reactor in this work. Similar conclusions were demonstrated by Li,[27] who reported that CaClOH and $CaCO_3$ were formed during the adsorption of CO_2/HCl mixtures by CaO

(a) 550 °C
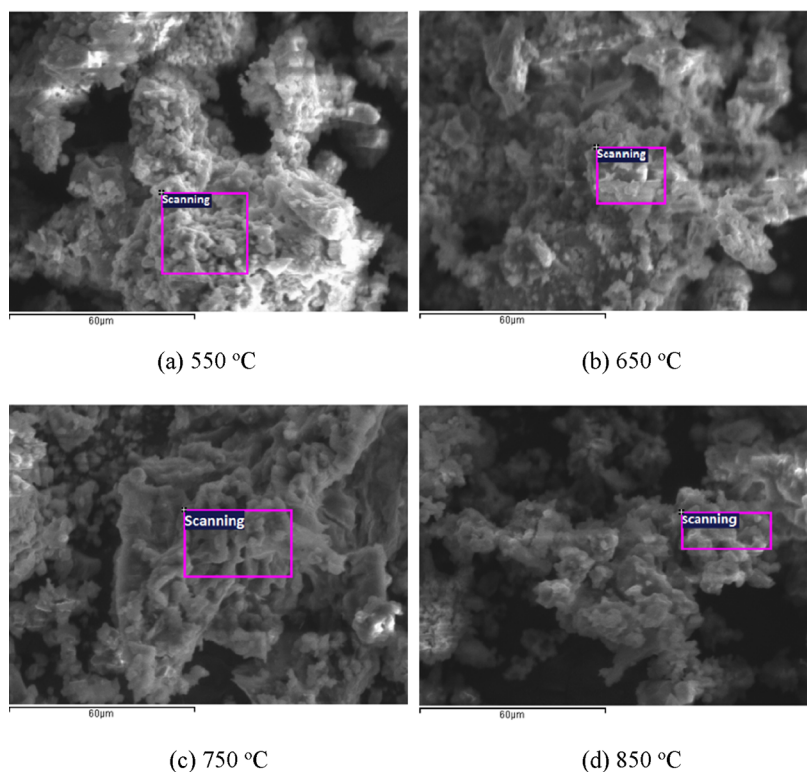
(b) 650 °C

(c) 750 °C

(d) 850 °C

Figure 10. SEM images of solid products at experimental temperatures: (a) 550; (b) 650; (c) 750; and (d) 850 °C.

reactant. Xie[48] had concluded that both CaClOH and CaCl$_2$ were dechlorination products by Ca-based additives. CaClOH was generated for a short dechlorination time (at dozens of minutes), whereas CaCl$_2$ was generated when the reaction time was long enough (at dozens of hours). Therefore, CaClOH has recorded as the main dechlorination product during the co-pyrolysis of waste biomass and plastic blends with the use of in situ CaO in this work.

Figure 10 shows the SEM characterization results of the solid productions. As presented, the surface of the solid products at the reaction temperature of 550 °C was looser and more porous compared to that at higher temperatures. With the increase in reaction temperature, the surface became denser and denser. At 750 °C, it was obviously melted and smoothed, indicating that the sintering and melting of the dechlorination products occurred at the reaction surface. The reason is, as aforementioned, mainly because the melting temperature of the dechlorination product, CaCl$_2$, was 772 °C. The SEM results confirmed that calcination and sintering of the reactants and the product layers at higher temperatures changed the surface properties of CaO, thus inhibiting the mitigation of HCl by CaO additive.

4. CONCLUSIONS

In this work, the effect of temperature and CaO addition on the co-pyrolysis of waste biomass and plastics were experimentally investigated in a fixed-bed tubular furnace reactor. Yields and properties of the produced fuel gas, tar cracking, and the mitigation efficiency of HCl gas by in situ CaO additive were determined. The results show that the temperature was the most critical factor determining the yields of three-phase products. Higher temperatures promoted the yield of fuel gas and reduced the production of condensate liquids and solid residues. With the increase in experimental temperature from 550 to 850 °C, the yield of fuel gas increased sharply by approximately 5.5 times from 81.9 to 451.4 mL/g-blends. With the addition of CaO, the total gas yield increased by 30.0−58.8 mL/g-blends. The content of tar was significantly reduced from 0.47 g/g-blends without CaO at 550 °C to 0.14 g/g-blends in the presence of CaO at 850 °C by thermal cracking and catalytic cracking of tar. Moreover, HCl was also immobilized into the solid residues by dechlorination reactions with the addition of CaO to generate CaClOH. From both the gas quality and HCl mitigation perspectives, the pyrolysis temperature of 750 °C and the Ca/Cl molecular ratio of 2/1 was found to be the optimum reaction condition with the HCl mitigation efficiency of 83.6%.

■ AUTHOR INFORMATION

Corresponding Author

Yuanjun Tang − Department of Energy and Environment System Engineering, Zhejiang University of Science and Technology, Hangzhou 310023, China; orcid.org/0000-0002-6467-2549; Email: tang@zust.edu.cn

Authors

Jun Dong − Zhejiang Energy R&D Institute Co., Ltd., Hangzhou 311121, China

Yuan Zhao − PowerChina HuaDong Engineering Co., Ltd., Hangzhou 311122, China

Guoneng Li − Department of Energy and Environment System Engineering, Zhejiang University of Science and Technology,

Hangzhou 310023, China; orcid.org/0000-0002-6366-3683

Yong Chi − State Key Laboratory of Clean Energy Utilization, Zhejiang University, Hangzhou 310027, China; orcid.org/0000-0001-6360-6198

Elsa Weiss-Hortala − Ecole des Mines d'Albi Carmaux, RAPSODEE Research Centre, Albi Cedex 09 81013, France

Ange Nzihou − Ecole des Mines d'Albi Carmaux, RAPSODEE Research Centre, Albi Cedex 09 81013, France

Guanqun Luo − Department of Energy and Environment System Engineering, Zhejiang University of Science and Technology, Hangzhou 310023, China; orcid.org/0000-0002-7931-2925

Chao Ye − Department of Energy and Environment System Engineering, Zhejiang University of Science and Technology, Hangzhou 310023, China

Complete contact information is available at:
https://pubs.acs.org/10.1021/acsomega.2c04279

Notes
The authors declare no competing financial interest.

■ ACKNOWLEDGMENTS

■ REFERENCES
(1) Ding, Y.; Zhao, J.; Liu, J.; Zhou, J.; Cheng, L.; Zhao, J.; Shao, Z.; Iris, Ç.; Pan, B.; Li, X.; Hu, Z. A review of China's municipal solid waste (MSW) and comparison with international regions: Management and technologies in treatment and resource utilization. *J. Clean. Prod.* **2021**, *293*, 126144.

(2) Wei, J.; Li, H.; Liu, J. Fate of dioxins in a municipal solid waste incinerator with state-of-the-art air pollution control devices in China. *Environ. Pollut.* **2021**, *289*, 117798.

(3) Zhu, J.; Hao, Q.; Chen, J.; Hu, M.; Tu, T.; Jiang, C. Distribution characteristics and comparison of chemical stabilization ways of heavy metals from MSW incineration fly ashes. *Waste Manag.* **2020**, *113*, 488−496.

(4) Song, Q.; Zhao, H.; Jia, J.; Yang, L.; Lv, W.; Bao, J.; Shu, X.; Gu, Q.; Zhang, P. Pyrolysis of municipal solid waste with iron-based additives: A study on the kinetic, product distribution and catalytic mechanisms. *J. Clean. Prod.* **2020**, *258*, 120682.

(5) Li, Q.; Yu, A.; Chen, S.; Tang, Y.; Ma, X.; Gholizadeh, M. Progress in catalytic pyrolysis of municipal solid waste. *Energy Convers. Manage.* **2020**, *226*, 113525.

(6) Trinh, V. T.; Jeong, T.-Y.; Lee, B.-H.; Jeon, C.-H. Comparative Study of the Synergistic Effects of Blending Raw/Torrefied Biomass and Vietnamese Anthracite Using Co-pyrolysis. *ACS Omega* **2021**, *6*, 29171−29183.

(7) Pihl, O.; Khaskhachikh, V.; Kravetskaja, J.; Niidu, A.; Siirde, A. Co-Pyrolysis of Estonian Oil Shale with Polymer Wastes. *ACS Omega* **2021**, *6*, 31658−31666.

(8) Wantaneeyakul, N.; Kositkanawuth, K.; Turn, S. Q.; Fu, J. Investigation of Biochar Production from Copyrolysis of Rice Husk and Plastic. *ACS Omega* **2021**, *6*, 28890−28902.

(9) Cao, C.; Bian, C.; Wang, G.; Bai, B.; Xie, Y.; Jin, H. Co-gasification of plastic wastes and soda lignin in supercritical water. *Chem. Eng. J.* **2020**, *388*, 124277.

(10) Zhu, H. L.; Zhang, Y. S.; Materazzi, M.; Aranda, G.; Brett, D. J. L.; Shearing, P. R.; Manos, G. Co-gasification of beech-wood and

polyethylene in a fluidized-bed reactor. *Fuel Process. Technol.* **2019**, *190*, 29−37.

(11) Bai, B.; Jin, H.; Zhu, S.; Wu, P.; Fan, C.; Sun, J. Experimental investigation on in-situ hydrogenation induced gasification characteristics of acrylonitrile butadiene styrene (ABS) microplastics in supercritical water. *Fuel Process. Technol.* **2019**, *192*, 170−178.

(12) Couto, N.; Monteiro, E.; Silva, V.; Rouboa, A. Hydrogen-rich gas from gasification of Portuguese municipal solid wastes. *Int. J. Hydrogen Energy* **2016**, *41*, 10619−10630.

(13) Gu, Q.; Wu, W.; Jin, B.; Zhou, Z. Analyses for Synthesis Gas from Municipal Solid Waste Gasification under Medium Temperatures. *Processes* **2020**, *8*, 84.

(14) Xu, M.; Zhu, X.; Li, X.; Hu, Z.; Huang, Y.; Xia, A.; Yao, H. Investigation of the combustion behaviors and kinetic modelling of municipal solid waste char under isothermal conditions using a micro-fluidized bed. *J. Environ. Chem. Eng.* **2021**, *9*, 105984.

(15) Xu, F.; Wang, B.; Yang, D.; Ming, X.; Jiang, Y.; Hao, J.; Qiao, Y.; Tian, Y. TG-FTIR and Py-GC/MS study on pyrolysis mechanism and products distribution of waste bicycle tire. *Energy Convers. Manage.* **2018**, *175*, 288−297.

(16) Prathiba, R.; Shruthi, M.; Miranda, L. R. Pyrolysis of polystyrene waste in the presence of activated carbon in conventional and microwave heating using modified thermocouple. *Waste Manag.* **2018**, *76*, 528.

(17) Kabir, G.; Hameed, B. Recent progress on catalytic pyrolysis of lignocellulosic biomass to high-grade bio-oil and bio-chemicals. *Renewable Sustainable Energy Rev.* **2017**, *70*, 945−967.

(18) Manyà, J. J.; Laguarta, S.; Ortigosa, M. A.; Manso, J. A. Biochar from Slow Pyrolysis of Two-Phase Olive Mill Waste: Effect of Pressure and Peak Temperature on its Potential Stability. *Energy Fuels* **2014**, *28*, 3271−3280.

(19) Policella, M.; Wang, Z.; Burra, K. G.; Gupta, A. K. Characteristics of syngas from pyrolysis and CO2-assisted gasification of waste tires. *Appl. Energy* **2019**, *254*, 113678.

(20) Mazlan, M. A. F.; Uemura, Y.; Osman, N. B.; Yusup, S. Fast pyrolysis of hardwood residues using a fixed bed drop-type pyrolyzer. *Energy Convers. Manage.* **2015**, *98*, 208−214.

(21) Robinson, J.; Binner, E.; Vallejo, D. B.; Perez, N. D.; Al Mughairi, K.; Ryan, J.; Shepherd, B.; Adam, M.; Budarin, V.; Fan, J.; Gronnow, M.; Peneranda-Foix, F. Unravelling the mechanisms of microwave pyrolysis of biomass. *Chem. Eng. J.* **2022**, *430*, 132975.

(22) Wan Mahari, W. A.; Awang, S.; Zahariman, N. A. Z.; Peng, W.; Man, M.; Park, Y.-K.; Lee, J.; Sonne, C.; Lam, S. S. Microwave co-pyrolysis for simultaneous disposal of environmentally hazardous hospital plastic waste, lignocellulosic, and triglyceride biowaste. *J. Hazard Mater.* **2022**, *423*, 127096.

(23) Beneroso, D.; Bermúdez, J. M.; Arenillas, A.; Menéndez, J. A. Integrated microwave drying, pyrolysis and gasification for valorisation of organic wastes to syngas. *Fuel* **2014**, *132*, 20−26.

(24) Zhang, X.; Lei, H.; Wang, L.; Zhu, L.; Wei, Y.; Liu, Y.; Yadavalli, G.; Yan, D. Renewable gasoline-range aromatics and hydrogen-enriched fuel gas from biomass via catalytic microwave-induced pyrolysis. *Green Chem.* **2015**, *17*, 4029−4036.

(25) Liu, H.; Ye, C.; Xu, Y.; Wang, Q. Effect of activation conditions and iron loading content on the catalytic cracking of toluene by biochar. *Energy* **2022**, *247*, 123409.

(26) Wang, M.; Qi, Y.; Ma, R.; Fu, Z.; Ge, P.; Ji, S.; Wu, J.; Qian, X. Investigation of CaO Influences on Fast Gasification Characteristics of Biomass in a Fixed-bed Reactor. *Waste Biomass Valorization* **2020**, *11*, 3731−3738.

(27) Li, Y.; Wang, W.; Cheng, X.; Su, M.; Ma, X.; Xie, X. Simultaneous CO2/HCl removal using carbide slag in repetitive adsorption/desorption cycles. *Fuel* **2015**, *142*, 21−27.

(28) Wang, J.; Zhao, B.; Zhu, D.; Huang, F.; Zhang, W.; Yang, H.; Chen, L.; Guan, H.; Sun, L.; Yang, S.; Xu, D.; Yan, B. Mechanism on catalytic cracking tar with CaO-based catalysts for hydrogen-rich gas by DFT and experiments. *Int. J. Hydrogen Energy* **2021**, *46*, 6522−6531.

(29) Al-Obaidi, M. M. A.; Ishak, N. S.; Ali, S.; Arifin, N. A.; Raja Shahruzzaman, R. M. H.; Wan Abdul Karim Ghani, W. A.; Hin, T. Y.; Shamsuddin, A. H. H-2-Rich and Tar-Free Downstream Gasification Reaction of EFB by Using the Malaysian Dolomite as a Secondary Catalyst. *Catalysts* **2021**, *11*, 447.

(30) Wang, B.; Li, X.; Wang, X.; Zhang, B. Effect of filling materials on CO2 conversion with a dielectric barrier discharge reactor. *J. Environ. Chem. Eng.* **2021**, *9*, 44.

(31) Wang, J.; Ma, M.; Bai, Y.; Su, W.; Song, X.; Yu, G. Effect of CaO additive on co-pyrolysis behavior of bituminous coal and cow dung. *Fuel* **2020**, *265*, 116911.

(32) Wei, L.; Xu, S.; Liu, J.; Liu, C.; Liu, S. Hydrogen production in steam gasification of biomass with CaO as a CO2 absorbent. *Energy Fuels* **2008**, *22*, 1997−2004.

(33) Zheng, X.; Ying, Z.; Wang, B.; Chen, C. Effect of Calcium Oxide Addition on Tar Formation During the Pyrolysis of Key Municipal Solid Waste (MSW) Components. *Waste Biomass Valorization* **2019**, *10*, 2309−2318.

(34) Zhang, Y.; Wang, J.; Lv, P.; Bie, N.; Cao, P.; Bai, Y.; Song, X.; Yu, G. Capture of released alkali metals and its simultaneously catalytic performance on secondary reactions of volatiles during biomass pyrolysis. *Fuel* **2022**, *317*, 123557.

(35) Efika, E. C.; Onwudili, J. A.; Williams, P. T. Products from the high temperature pyrolysis of RDF at slow and rapid heating rates. *J. Anal. Appl. Pyrol.* **2015**, *112*, 14−22.

(36) Li, A. M.; Li, X. D.; Li, S. Q.; Ren, Y.; Chi, Y.; Yan, J. H.; Cen, K. Pyrolysis of solid waste in a rotary kiln: influence of final pyrolysis temperature on the pyrolysis products. *J. Anal. Appl. Pyrol.* **1999**, *50*, 149−162.

(37) Özbay, N.; Pütün, A. Pyrolysis of peach pulp: effect of chemical additives. *Energy Sources, Part A* **2014**, *36*, 2546−2554.

(38) Li, X.; Tang, Y.; Zhao, Y.; Li, G.; Luo, G.; Wang, W.; Ye, C.; Xu, Y. Dual effect of CaO on waste PVC plastics pyrolysis: A kinetics study using Fraser-Suzuki deconvolution. *Thermochim. Acta* **2022**, *715*, 179295.

(39) Shang, S.; Qin, Z.; Lan, K.; Wang, Y.; Zhang, J.; Xiong, T.; He, W.; Li, J. Hydrogen-rich Syngas Production via Catalytic Gasification of Biomass Using Ni/Zr-MOF Catalyst. *Bioresources* **2020**, *15*, 1716−1731.

(40) Han, L.; Wang, Q.; Yang, Y.; Yu, C.; Fang, M.; Luo, Z. Hydrogen production via CaO sorption enhanced anaerobic gasification of sawdust in a bubbling fluidized bed. *Int. J. Hydrogen Energy* **2011**, *36*, 4820−4829.

(41) De Filippis, P.; Borgianni, C.; Paolucci, M.; Pochetti, F. Prediction of syngas quality for two-stage gasification of selected waste feedstocks. *Waste Manag.* **2004**, *24*, 633−639.

(42) Dong, J.; Nzihou, A.; Chi, Y.; Weiss-Hortala, E.; Ni, M.; Lyczko, N.; Tang, Y.; Ducousso, M. Hydrogen-Rich Gas Production from Steam Gasification of Bio-char in the Presence of CaO. *Waste Biomass Valorization* **2017**, *8*, 2735−2746.

(43) Irfan, M.; Li, A.; Zhang, L.; Ji, G.; Gao, Y. Catalytic gasification of wet municipal solid waste with HfO2 promoted Ni-CaO catalyst for H2-rich syngas production. *Fuel* **2021**, *286*, 119408.

(44) Lazzarotto, I. P.; Ferreira, S. D.; Junges, J.; Bassanesi, G. R.; Manera, C.; Perondi, D.; Godinho, M. The role of CaO in the steam gasification of plastic wastes recovered from the municipal solid waste in a fluidized bed reactor. *Process Saf. Environ.* **2020**, *140*, 60−67.

(45) Shemwell, B.; Levendis, Y. A.; Simons, G. A. Laboratory study on the high-temperature capture of HCl gas by dry-injection of calcium-based sorbents. *Chemosphere* **2001**, *42*, 785−796.

(46) Li, Y.; Ma, X.; Wang, W.; Chi, C.; Shi, J.; Duan, L. Enhanced CO2 capture capacity of limestone by discontinuous addition of hydrogen chloride in carbonation at calcium looping conditions. *Chem. Eng. J.* **2017**, *316*, 438−448.

(47) Samantray, J.; Anand, A.; Dash, B.; Ghosh, M. K.; Behera, A. K. Production of Potassium Chloride from K-Feldspar Through Roast-Leach-Solvent Extraction Route. *Trans. Indian Inst. Met.* **2019**, *72*, 2613−2622.

(48) Xie, X.; Li, Y.; Wang, W.; Shi, L. HCl removal using cycled carbide slag from calcium looping cycles. *Appl. Energy* **2014**, *135*, 391−401.